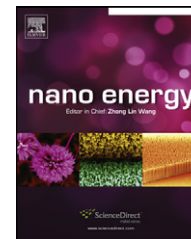


Available online at www.sciencedirect.com**SciVerse ScienceDirect**journal homepage: www.elsevier.com/locate/nanoenergy

Graphene/Si multilayer structure anodes for advanced half and full lithium-ion cells

Liwen Ji^a, Honghe Zheng^b, Ariel Ismach^a, Zhongkui Tan^a, Shidi Xun^b, Eric Lin^a, Vincent Battaglia^b, Venkat Srinivasan^b, Yuegang Zhang^{a,*}

^aThe Molecular Foundry, Lawrence Berkeley National Laboratory, Berkeley, CA 94720, USA

^bAdvanced Energy Technology Department, Lawrence Berkeley National Laboratory, Berkeley, CA 94720, USA

KEYWORDS

Graphene/Si multilayer structures; Lithium-ion half cells and full cells

Abstract

Graphene/Si multilayer structures were constructed through a repeated process of filtering liquid-phase exfoliated graphene film and the subsequent coating of amorphous Si film via plasma-enhanced chemical vapor deposition (PECVD) method. The multilayer heterogeneous structure films, directly fabricated on copper current collectors, were used as anodes for rechargeable lithium half-cells and full-cells without adding any polymer binder or conductive additives. The half cells based on the new anodes could easily achieve a capacity almost four times higher than the theoretical value of graphite even after 30 cycles' charging/discharging. It also demonstrated improved capacity retention compared to those of pure Si film-based anodes. Furthermore, full cells composed of the graphene/Si multilayer structure anodes and commercially available $\text{LiNi}_{1/3}\text{Mn}_{1/3}\text{Co}_{1/3}\text{O}_2$ cathodes were also assembled. Initial results showed good electrochemical performance comparable to that of commercially available rechargeable LIBs. Our prepared multilayer structures, taking advantage of the long cycle life of carbon and the high lithium-storage capacity of Si, provided a promising research platform that may eventually lead to an optimized anode structure for advanced rechargeable LIBs.

© 2011 Published by Elsevier Ltd.

1. Introduction

Si-based electrodes for rechargeable lithium-ion batteries (LIBs) have attracted considerable attention. As a naturally abundant element, Si has the highest theoretical specific

capacity among all existing anodes, which can reach 4200 mAh g^{-1} in the form of $\text{Li}_{4.4}\text{Si}$ [1-6]. Unfortunately, its potential in broad commercial applications has been hindered by severe capacity fading and loss of electrical contact caused by huge volume change, structural crumbling and cracking during repeated charging/discharging, especially at high currents. Downsizing from conventional bulk to various nanoscale morphologies/structures or dispersing these nanostructured Si into carbon matrices are the most appealing approaches being pursued to overcome these issues and to improve the

*Corresponding author. Tel.: +1 510 486 5282; fax: +1 510 486 6166.

E-mail address: yzhang5@lbl.gov (Y. Zhang).

overall electrochemical performance of Si-based anodes in rechargeable LIBs [1-6]. Here, the size reduction can help to accommodate the volume change, facilitate more efficient electronic/ionic diffusion and provide more active sites, while the carbon component in the Si/carbon nanocomposites can create a conducting matrix to maintain the electrical contact of the electrode with the current collector, resulting in better endurance to the huge stresses during continuous charge/discharge cycling and enhance structural flexibility. In addition, the incorporation of Li-active Si into carbon-based electrodes can reduce the initial irreversible capacity, improve both the Coulombic efficiency and cycling performance of electrodes [1-6].

Graphene is a new class of monolayer of carbon atoms densely packed in a honeycomb crystal lattice. Owing to its exceptional properties including extraordinarily electronic and thermal properties, amazing mechanical strength, ultra-high surface area [6,7], graphene could be superior to other carbon materials as a conductive matrix to enhance electron transport and electrical contact with Si active materials in rechargeable LIBs and to effectively prevent the volume expansion/shrinkage and aggregation of Si phases during the Li charge/discharge processes. Furthermore, its large surface

area could also facilitate the absorption of Li atoms on both sides of the graphene sheet or into its ubiquitous cavities. As a result, graphene-based materials have attracted unmatched attention and has also triggered tremendous experimental activities for applications in next generation electronic and energy storage devices [6,8-14]. Recently, Chou et al. blended commercially available nanosized Si particles and graphene to prepare eco-friendly and low cost LIB anodes, which exhibited enhanced cycling stability [15]. In the meantime, other groups also successfully prepared Si nanoparticles/graphene paper composite as anodes for rechargeable LIBs with high Li storage capability and cycling stability [8,16]. Although these progress, there are still no reports about constructed graphene-Si based multilayer structures and there are also no reports about evaluating the electrochemical performance of graphene/Si nanocomposites in Li-ion full cells. Because of these fascinating heterogeneous architectures, there may have some charming electrochemical performance in rechargeable LIBs.

In this work, we designed graphene/Si multilayer structures by filtering liquid phase exfoliated graphene the subsequent PECVD coating Si process (a schematic is provided in Fig. 1(a)). In this judiciously fabricated nanostructure, the

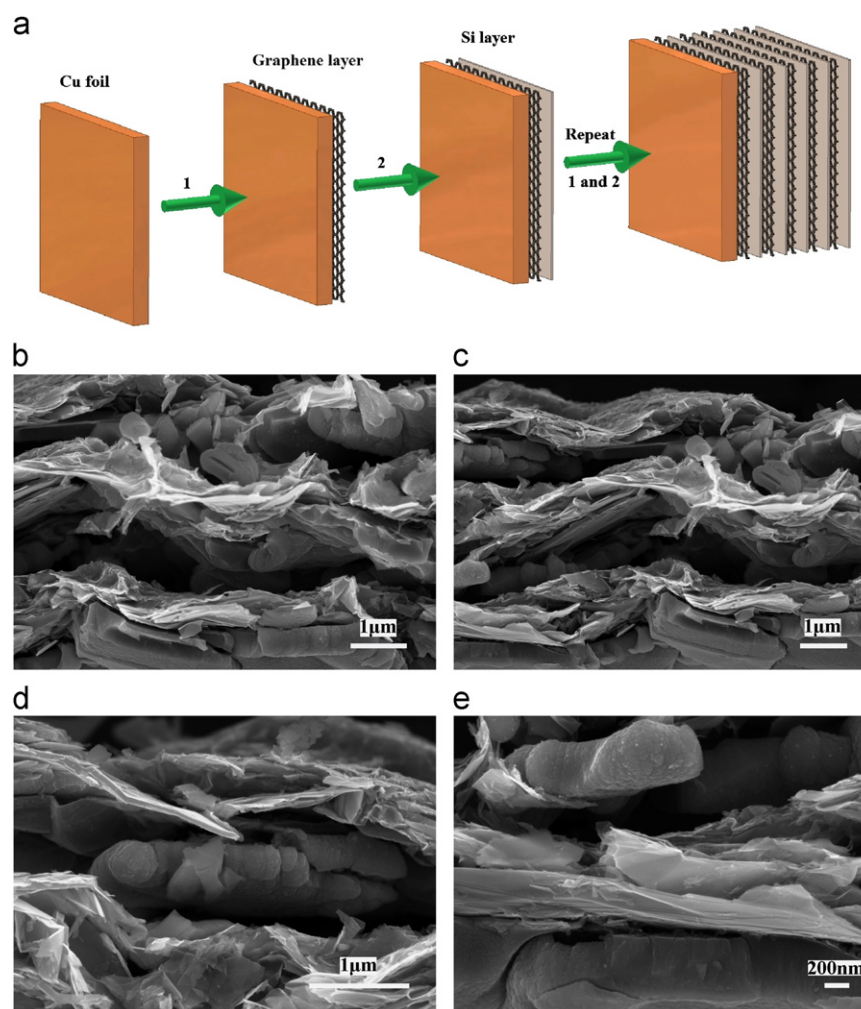


Figure 1 (a) Schematic illustration of preparation procedures of graphene/Si multilayer structures; and (b-e) cross-sectional SEM images of multilayer graphene/Si structures: (b) and (c) repeated graphene/Si layer structures, (d) graphene-Si-graphene structures, and (e) Si-graphene-Si structures.

flexible graphene films were designed to buffer the structural changes caused by volume expansion and extraction of Si layers during the Li alloying/de-alloying processes. In addition, the graphene-film layers could isolate each Si layer, circumventing the Si aggregation problem. As a result, this facile approach can provide optimizing graphene/Si nano-architectures where the graphene layers function as flexible mechanical support to mitigate and accommodate the volumetric-change-induced stresses/strains in the Si layer and therefore, can alleviate or even avoid the pulverization of Si phase, maintaining the structural integrity of the electrodes at the same time. In addition, this reinforcing material offers an efficient, electrically conducting medium and effectively improves the adhesion strength between different active materials and also with Cu foil current collector. As a result, these binder-free graphene/Si multilayer structure anodes exhibit a high reversible capacity and good capacity retention in both Li half cells and full cells.

2. Material and methods

2.1. Materials

Graphite powder, N-methyl-2-pyrrolidone (NMP), and sodium hydroxide (NaOH) were purchased from Sigma-Aldrich. Anodic aluminum oxide (AAO) membrane was obtained from Whatman. Graphite was dispersed in NMP solvent for sonicating using bath sonication equipment. The resultant dispersion was then centrifuged and decantation was carried out by pipetting off the top half of the dispersion [17].

2.2. Preparations for graphene/Si multilayer structures

The prepared graphene NMP solution was filtrated directly using AAO membrane. The vacuum filtration of the as-prepared graphene dispersions in NMP resulted in the formation of graphene films on the AAO membrane. After removing the AAO membrane with NaOH solution and repeated rinsing with distilled water, these thin graphene films with a thickness of about 500 nm were directly transferred to copper foil-based current collectors. Afterwards, the Si films were deposited on the as-prepared graphene film surface via a PECVD process with 10% SiH₄ in Ar as precursors. Subsequently, the same processes were repeated to prepare graphene/Si multilayer structures. Using the as-described filtration or PECVD process, we also prepared pure graphene and PECVD Si films on copper foils.

2.3. Characterizations

The samples were characterized by scanning electron microscopy (SEM: Zeiss Gemini Ultra-55) with energy dispersive X-ray spectroscopy (EDS), X-ray diffraction (Diffraktometer D500/501, Siemens), and Raman spectroscopy (Witec with a 532 nm green laser).

2.4. Electrochemical measurements

2032 coin-type half cells were assembled with the prepared graphene/Si multilayer structures, pure graphene films, and PECVD Si films as the anodes in a high-purity argon-filled glove box. Thin Li foils were employed as the counter electrodes and polypropylene membranes were used as the separator. The electrolyte used was 1 M lithium hexafluorophosphate (LiPF₆), dissolved in 1/1 (V/V) ethylene carbonate (EC)/ethyl methyl carbonate (EMC). 2032 coin-type full cells with commercially available LiNi_{1/3}Mn_{1/3}Co_{1/3}O₂ as cathodes and the graphene/Si multilayer structures as anodes were also assembled in a high-purity argon-filled glove box. The tested cathodes were prepared by mixing LiNi_{1/3}Mn_{1/3}Co_{1/3}O₂, carbon black, and polyvinylidene difluoride (PVDF) at a weight ratio of 80:10:10 in NMP solvent to form a slurry. The resultant slurry was uniformly pasted on pure alumina foil and dried firstly at room temperature for 12 h and then at 130 °C for 16 h. Galvanostatic charge and discharge experiments of the half cells and full cells were conducted using an Arbin automatic battery cyler at several different current densities between cut-off potentials of 0.002 and 2.80 V for half cells and 3.0-4.3 V for full cells.

3. Results and discussion

As described in the experimental sections, we obtained graphene film via filtering liquid phase exfoliated graphene (Raman spectra in Fig. S1 indicates that the few-layer graphene flakes in the prepared film are completely different with the starting graphite powers. This is also consistent with the formerly reported results [17].); subsequently, the graphene film was directly transferred to copper foil. Then a Si film was deposited onto the graphene film surface via PECVD process (X-Ray diffraction pattern in Fig. S2 indicates the PECVD Si film is amorphous). The as-prepared graphene/Si layered structure is defined as one layer graphene/Si structure hereafter. Finally, such filtering-transferring and PECVD processes were repeated three or five times to prepare three-layered or five-layered graphene/Si structures.

The morphologies and microstructures of as-prepared graphene film, PECVD Si film, and the graphene/Si multilayer structures were investigated by SEM. Fig. S3(a) and (b) show the morphology of a pure graphene film. Both micro-scale and submicron-scale sheets are present in the film, which pile up randomly. The morphology of the pure PECVD Si film is shown in Fig. S3(c) and (d). The film is amorphous and composed of small and large clusters. The uneven and roughened surface could have been inherited from the underlying copper foil. Fig. S3(e) and (f) are the planar-view SEM images of the as-prepared graphene/Si multilayer structures. The corresponding EDS analysis (see supporting information in Fig. S4) confirms the existence of the Si phase in the prepared graphene/Si multilayer structures, indicating that the PECVD Si films were coated on the graphene film. A comparison of Fig. S3(a) and (b) with (e) and (f) clearly shows that the top-layer Si film in the multilayer structure inherited the exact surface morphology of the underlying graphene flakes. In contrast to the rough

surface of Si coated onto copper foil, the Si coating on graphene sheets is very smooth and conformal, indicating good adhesion of Si onto the graphene film surface.

The alternating graphene films and Si layers of the multilayer samples are clearly shown in the cross-sectional SEM images in Fig. 1(b-e). The graphene sheets are loosely stacked into continuous films without apparent stacking order. Voids of different sizes along with a large amount of cavities and defects can be observed in both the graphene layer and the Si layer (note that some big cracks between graphene films and Si layers were introduced by the cutting process during the preparation of the cross-sectional SEM samples). The measured single layer thickness for both graphene and Si films is about 500 nm, consistent with their nominal values. As a result, the as-formed five, three, and one layer graphene/Si structures should have thickness at around 1, 3, and 5 μm , respectively.

The obtained graphene/Si multilayer structures (including five layers, three layers, and one layer), containing about 56 wt% Si and 34 wt% graphene, were directly used as binder-free anodes for Li half cells. Fig. 2(a) displays typical cyclic voltammogram (CV) curve of a half cell with a five layer graphene/Si structure as anode. It is noted that the first cycle reduction scanning curve was significantly suppressed and only has a weak and broad peak, while the first cycle oxidation scanning curve has a clear peak at about 0.6 V. Two new reduction peaks at 0.2/0.3 V and another new oxidation peak at about 0.45 V appeared at the second cycle redox scanning curve. In the subsequent cycles, these oxidation/reduction peaks settled rapidly and maintained a

steady pattern eventually resulting in the peaks overlapping one another; it is noted that this phenomena is similar to that of the pure Si film anodes (Fig. S5). The initial flat reduction curve at the first cycle could be due to the formation of a solid electrolyte interface (SEI) film on the surface of the electrodes and could also be due to the initially inactivated surface acting against the electrochemical reaction. During the subsequent cycles, several peaks were recognized on potential scanning branches toward both anodic and cathodic potentials. These peaks were attributed to the potential dependent formation and disappearance of Li-Si alloys with different compositions [18-29].

Fig. 2(b) displays the charge/discharge profiles at C/40 (50 mA g^{-1}) with a potential window from 0.002 V to 2.8 V for a half cell. It is remarkable to note that a very high first cycle charge/discharge capacity value of about 2499 and 2217 mAh g^{-1} was obtained, corresponding to a high Coulombic efficiency of about 88.71%, which is larger than the previously reported results for carbon/Si anodes [16,30]. The irreversible capacity ratio of 11.29% can be assigned to the reductive decomposition of the electrolyte, forming a SEI film on the electrode surface [16,30]. It was also noted that during the first charge process, the voltage steeply decreased to about 0.20-0.30 V, followed by a slow decrease to 0.002 V. During the subsequent cycles, the charging/discharging profiles showed smooth sloping curves. These phenomena are consistent with the previously reported electrochemical behavior of Si-based anodes [1-4,16,30]. During the second cycle, these materials delivered a reversible capacity of 2163 mAh g^{-1} , corresponding to a

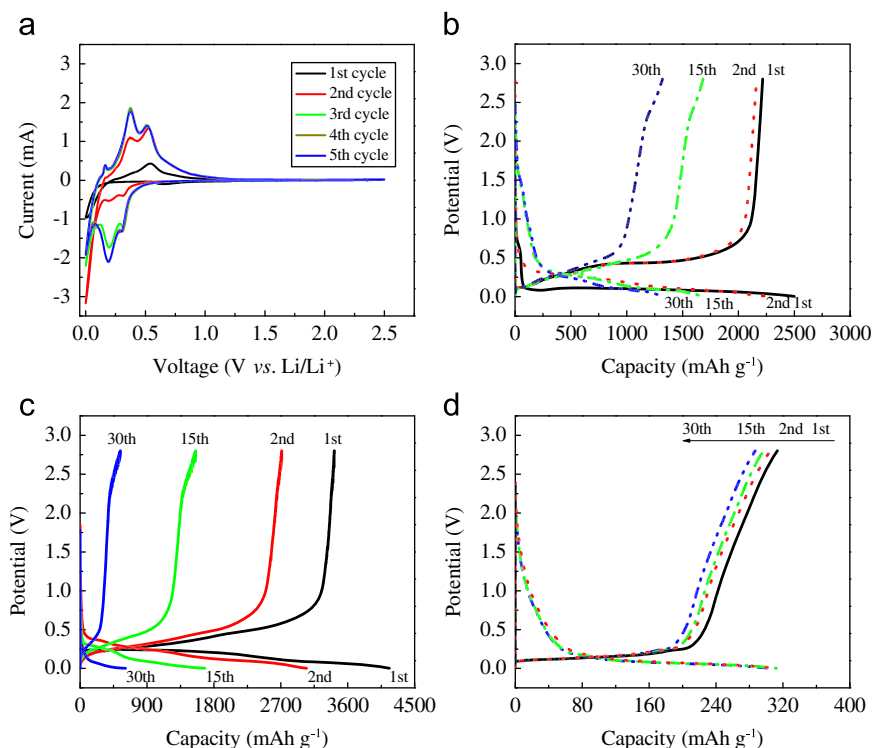


Figure 2 (a) CV curve of a five-layer graphene/Si structure anode with 0.1 mV s^{-1} scanning rate in the potential window from 2.8 V to 0.002 V. Galvanostatic charge/discharge profiles of (b) five-layer graphene/Si structures, (c) pure PECVD Si films, and (d) pure graphene films at a cycling rate of C/40 with a cutoff voltage window of 2.8-0.002 V.

97.6% capacity retention. In addition, a large Coulombic efficiency of about 96% was obtained at the second cycle, and this value was also preserved in subsequent cycles. At the 15th and 30th cycles, the discharge capacities were about 1683 and 1320 mAh g⁻¹, respectively, retaining 75.9% and 59.5% of the initial value.

For comparison, the electrochemical evaluations of both the pure graphene and PECVD Si films were also carried out. The results are displayed in Fig. 2(c) and (d). The pure Si film exhibited near theoretical charge/discharge capacities of about 4159 and 3418 mAh g⁻¹ at the first cycle with a Coulombic efficiency of about 82.18% (Fig. 2(c)). After that, the capacity began to fade dramatically. For example, at the second cycle, the discharge capacity decreased to 2712 mAh g⁻¹, a 79.3% capacity retention of the first cycle value. At the 15th and 30th cycles, the reversible capacity can only be preserved at about 1554 and 541 mAh g⁻¹, respectively, indicating only 45.5% and 15.8% capacity retention of the initial value. The pure graphene film anode had a relatively lower reversible capacity of about 313 mAh/g at the first cycle, but good capacity retention (the value was about 287 mAh g⁻¹ at the 30th cycle) (Fig. 2(d)), which is similar to other reported results [31].

In our graphene/Si multilayer structures, the Si thin-films were confined between the graphene layers, which serve as structural buffers to relax the huge mechanical stress induced during cycling and prevent continuous fragmentation, and aggregation of Si so that the excellent structural and electrical integrity of the electrodes was preserved. As a result, our graphene/Si multilayer structures demonstrated improved cycle life.

To understand the influence of the number of graphene/Si layers on capacity retention, we also measured the charge/discharge profiles of three layers and one layer graphene/Si structure anodes under the same conditions. The results are summarized in Fig. 3(a) and (b). Both samples showed large reversible capacities of 2023 and 2098 mAh g⁻¹ at the first cycle, with corresponding Coulombic efficiencies of about 81.3% and 82.0%, respectively. These values are comparable to the five-layer graphene/Si anodes. At the second cycle, these materials had reversible capacities of about 1809 and 1804 mAh g⁻¹, representing about 89.4 and 86.0% capacity retentions compared with their first cycle values. These reversible capacities decreased to 1181 and 848 mAh g⁻¹ at the 30th cycle, indicating 58.1% and 40.4% capacity

retention of their first cycle values. These results may suggest that the capacity fading of graphene/Si multilayer structures can be further reduced by increasing the number of graphene/Si layers.

In order to demonstrate the high-rate capability of the graphene/Si multilayer structures, we performed cycle performance tests at various charge/discharge rates. Fig. S6(a) and (b) shows the rate capability results of five-layer graphene/Si structures. In Fig. S6(a), we found that the discharge capacity at C/10 was 2326 mAh g⁻¹ at the first cycle and dropped to 2205 mAh/g at the 5th cycle at the same rate. The discharge capacity at C/2 started with a high value of 1821 mAh g⁻¹ as well as a high Coulombic efficiency of 96.5%. This value slowly decreased to 865 mAh g⁻¹ after 30 cycles. The subsequent charge/discharge process at C/10 lead back to a reversible capacity of 1526 mAh g⁻¹. Fig. S6(b) shows the galvanostatic rate capability of another five layer graphene/Si structure-base anode in a half-type coin cell. At a C/20 rate, the material could deliver a large first cycle discharge capacity of about 2218 mAh g⁻¹. After the cell was cycled at this rate for 5 cycles, the C-rate was increased stepwise to C/4, C/2, and 1C. Under these rates, the graphene/Si multilayer anode had an initial reversible capacity of about 1801, 1271, and 627 mAh g⁻¹. Decreasing the C-rate back to C/2 and C/4 caused the initial reversible capacity to increase back to 883 and 1354 mAh g⁻¹, respectively, showing reasonably good high-rate capability, which could be improved via further optimization. As far as we know, such detailed cycle performance and rate capability explorations have not been reported in other published results of graphene/Si-based anodes [8,15,16].

It has been reported that in pure Si film-based anodes, the continuously large volume changes always accompanying charging/discharging processes leads to the agglomeration of Si and causes microstructure changes that gradually destroy the electrical contact of the Si films with the current collector [21,25]. As a result, severe capacity fading follows. In comparison, our graphene/Si multilayer structures have at least three unique features. Firstly, the flexible and conductive graphene-film layers can suppress local stress gradients, accommodate the large volume expansions/shrinkages during a lithiation/delithiation process, and alleviate the aggregation and pulverization problems connected with pure Si [8,15,16]. Secondly, the robust

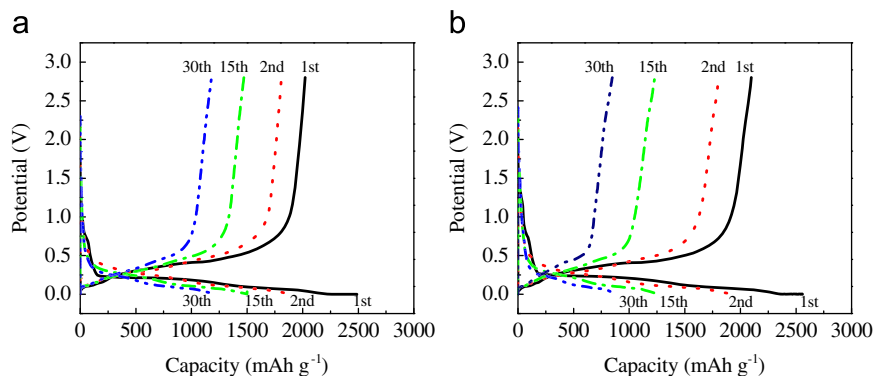


Figure 3 Galvanostatic charge/discharge profile of (a) three-layer graphene/Si structures, and (b) one-layer graphene/Si structures at a cycling rate of C/40 with a cutoff voltage window of 2.8-0.002 V.

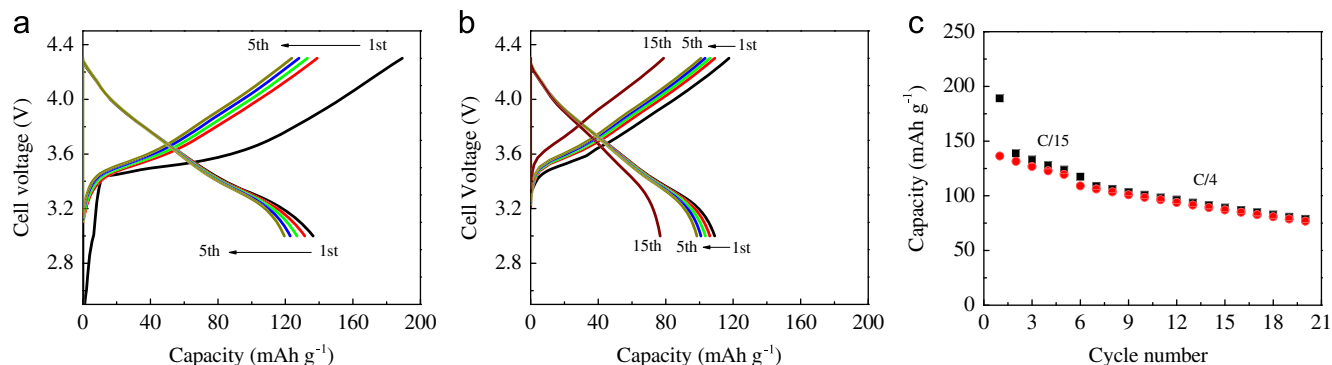


Figure 4 Voltage profiles of a full cell using a $\text{LiNi}_{1/3}\text{Mn}_{1/3}\text{Co}_{1/3}\text{O}_2$ cathode and a five-layer graphene/Si structured anode, with an initial cycling rate of C/15 for 5 cycles (a), followed by a continuous 15 cycles at C/4 (b), and the corresponding cycling performance curve (c). The specific capacity is calculated according to the mass of $\text{LiNi}_{1/3}\text{Mn}_{1/3}\text{Co}_{1/3}\text{O}_2$ cathode.

electrode architecture maintains good adhesion to the copper substrate, while additional graphene and Si layers can also remain anchored for adequate electrical continuity. Thirdly, the excellent electrical conductivity of graphene components ensures their good electrical contact with the adjacent Si films. These special structures with a large amount of void space between graphene flakes provide more reaction sites to facilitate the accessibility of the electrolyte and favor the rapid diffusion of both Li-ions and electrons during charge and discharge [9,14,18,19]. As a research platform, our filtration-PECVD combined approach is highly effective, simple, low cost and environment-friendly, and it also avoid the use of harsh oxidative process and harmful chemical reagents in most of approaches to make graphene/Si composites using reduced graphene oxide. Therefore, this approach opens an efficient new avenue for investigation of new carbon/semiconductor or metal multilayer structures electrodes for rechargeable LIBs.

As a final step to demonstrate its practical application, we assembled a Li-ion full cell using commercially available $\text{LiNi}_{1/3}\text{Mn}_{1/3}\text{Co}_{1/3}\text{O}_2$ as the cathode and the five layer graphene/Si structures as the anode and evaluated the electrochemical performance. To our knowledge, there is still no prior published study using graphene/Si composites as anodes in a full cell. Fig. 4 demonstrates the voltage profiles and the corresponding cycling performance of the five layer graphene/Si anodes in the full cell, where the specific capacities are calculated according to the mass of $\text{LiNi}_{1/3}\text{Mn}_{1/3}\text{Co}_{1/3}\text{O}_2$ -based cathodes.

The cycling rate used in the initial five cycles was C/15 and C/4 for the following 15 cycles. Here, $1\text{C}=180\text{ mA g}^{-1}$ according to the previously measured capacity of the $\text{LiNi}_{1/3}\text{Mn}_{1/3}\text{Co}_{1/3}\text{O}_2$ -based cathodes. From the charging/discharging curves in Fig. 4(a), it is apparent that the specific capacity, according to the weight of $\text{LiNi}_{1/3}\text{Mn}_{1/3}\text{Co}_{1/3}\text{O}_2$ -based cathodes, was 137 mAh g^{-1} , with an initial Coulombic efficiency of 72.05% at C/15; the specific capacity and Coulombic efficiency were about 120.0 mAh g^{-1} and 97.7%, respectively, at the 5th cycle under the same rate. After that, the cycling rate was increased to C/4, and the specific capacity could still be preserved at about 109 mAh g^{-1} after the first cycle with a high Coulombic efficiency of 92.8% (Fig. 4(b)). After 15 cycles at this C rate, the full cell still has a specific capacity of 77 mAh g^{-1} , indicating relatively good capacity retention of about 70.4%.

The cycle performance of the multilayer graphene/Si structures/ $\text{LiMn}_{1/3}\text{Co}_{1/3}\text{Ni}_{1/3}\text{O}_2$ full cell at C/15 (initial five cycles) and C/4 (the following 15 cycles) is shown in Fig. 4(c). These results show a gently sloping curve, indicating relatively good capacity retention. In addition, the cycle life curve shows that after the initial six cycles, these prepared full cells have very high Coulombic efficiency.

4. Conclusion

In summary, Graphene/Si multilayer structures were constructed *via* judicious and facile strategies of filtrating liquid-phase exfoliated graphene films and PECVD of Si films. These graphene/Si alternating multilayered structures were used as binder-free anodes for rechargeable LIBs and exhibited a large reversible capacity along with improved cycling characteristics. It was demonstrated that the highly compliant and flexible graphene layers could offer enhanced stress and strain resilience during charge/discharge cycling and thereby improve the structural stability and integrity of the composite anodes. This ductile graphene matrix also served as an interfacial adhesion layer and provided an efficient electrical conducting pathway and mechanical support to prevent capacity fading by keeping good electrical contact between the different layers. Our strategy incorporated dissimilar functional materials into one entity that provides the advantages of short lithium-ion diffusion pathways, large surface areas, and extremely appealing surface activities, allowing improved rate capabilities and cyclic characteristics. Further investigation based on such platform structures could lead to improved LIBs with more stable cycle life along with much faster charge-discharge kinetics.

Acknowledgments

This work was supported by the Office of Science, Office of Basic Energy Sciences, of the U.S. Department of Energy under Contract no. DE-AC02-05CH11231.

Appendix A. Supplementary material

Supplementary data associated with this article can be found in the online version at doi:10.1016/j.nanoen.2011.08.003.

References

- [1] C.K. Chan, H. Peng, G. Liu, K. McIlwrath, X.F. Zhang, R.A. Huggins, Y. Cui, *Nature Nanotechnology* 3 (2008) 31-35.
- [2] L. Ji, X. Zhang, *Energy & Environmental Science* 3 (2010) 124-129.
- [3] U. Kasavajjula, C. Wang, A.J. Appleby, *Journal of Power Sources* 163 (2007) 1003-1039.
- [4] R. Teki, M.K. Datta, R. Krishnan, T.C. Parker, T.M. Lu, P.N. Kumta, N. Koratkar, *Small* 5 (2009) 2236-2242.
- [5] L. Hu, H. Wu, Y. Gao, A. Cao, H. Li, J. McDough, X. Xie, M. Zhou, Y. Cui, *Advanced Energy Materials* 1 (2011) 523-527.
- [6] L. Ji, Z. Lin, M. Alcoutlabi, X. Zhang, *Energy & Environmental Science* 4 (2011) 2682-2699.
- [7] W. Choi, I. Lahiri, R. Seelaboyina, Y.S. Kang, *Critical Reviews in Solid State and Materials Sciences* 35 (2010) 52-71.
- [8] J.-Z. Wang, C. Zhong, S.-L. Chou, H.-K. Liu, *Electrochemistry Communications* 12 (2010) 1467-1470.
- [9] Z.-S. Wu, W. Ren, L. Wen, L. Gao, J. Zhao, Z. Chen, G. Zhou, F. Li, H.-M. Cheng, *ACS Nano* 4 (2010) 3187-3194.
- [10] L. Ji, Z. Tan, T. Kuykendall, E.J. An, Y. Fu, V. Battaglia, Y. Zhang, *Energy & Environmental Science* 4 (2011) 3611-3616.
- [11] L. Ji, Z. Tan, T.R. Kuykendall, S. Aloni, S. Xun, E. Lin, V. Battaglia, Y. Zhang, *Physical Chemistry Chemical Physics* 13 (2011) 7170-7177.
- [12] D. Wang, R. Kou, D. Choi, Z. Yang, Z. Nie, J. Li, L.V. Saraf, D. Hu, J. Zhang, G.L. Graff, J. Liu, M.A. Pope, I.A. Aksay, *ACS Nano* 4 (2010) 1587-1595.
- [13] H. Wang, L.-F. Cui, Y. Yang, H. Sanchez Casalongue, J.T. Robinson, Y. Liang, Y. Cui, H. Dai, *Journal of the American Chemical Society* 132 (2010) 13978-13980.
- [14] G. Zhou, D.-W. Wang, F. Li, L. Zhang, N. Li, Z.-S. Wu, L. Wen, G.Q. Lu, H.-M. Cheng, *Chemistry of Materials* 22 (2010) 5306-5313.
- [15] S.-L. Chou, J.-Z. Wang, M. Choucair, H.-K. Liu, J.A. Stride, S.-X. Dou, *Electrochemistry Communications* 12 (2010) 303-306.
- [16] J.K. Lee, K.B. Smith, C.M. Hayner, H.H. Kung, *Chemical Communications* 46 (2010) 2025-2027.
- [17] Y. Hernandez, V. Nicolosi, M. Lotya, F.M. Blighe, Z. Sun, S. De, I.T. McGovern, B. Holland, M. Byrne, Y.K. Gun'Ko, J.J. Boland, P. Niraj, G. Duesberg, S. Krishnamurthy, R. Goodhue, J. Hutchison, V. Scardaci, A.C. Ferrari, J.N. Coleman, *Nature Nanotechnology* 3 (2008) 563-568.
- [18] J. Rong, C. Masarapu, J. Ni, Z. Zhang, B. Wei, *ACS Nano* 4 (2010) 4683-4690.
- [19] S. Ohara, J. Suzuki, K. Sekine, T. Takamura, *Journal of Power Sources* 119-121 (2003) 591-596.
- [20] M.K. Datta, P.N. Kumta, *Journal of Power Sources* 158 (2006) 557-563.
- [21] V. Baranchugov, E. Markevich, E. Pollak, G. Salitra, D. Aurbach, *Electrochemistry Communications* 9 (2007) 796-800.
- [22] R.A. Huggins, *Journal of Power Sources* 81-82 (1999) 13-19.
- [23] Y. Yu, L. Gu, C. Zhu, S. Tsukimoto, P.A. van Aken, J. Maier, *Advanced Materials* 22 (2010) 2247-2250.
- [24] W.-R. Liu, Z.-Z. Guo, W.-S. Young, D.-T. Shieh, H.-C. Wu, M.-H. Yang, N.-L. Wu, *Journal of Power Sources* 140 (2005) 139-144.
- [25] K.-L. Lee, J.-Y. Jung, S.-W. Lee, H.-S. Moon, J.-W. Park, *Journal of Power Sources* 129 (2004) 270-274.
- [26] H.-C. Shin, J.A. Corno, J.L. Gole, M. Liu, *Journal of Power Sources* 139 (2005) 314-320.
- [27] X. Wang, Z. Wen, Y. Liu, X. Xu, J. Lin, *Journal of Power Sources* 189 (2009) 121-126.
- [28] C.J. Wen, R.A. Huggins, *Journal of Solid State Chemistry* 37 (1981) 271-278.
- [29] T. Takamura, S. Ohara, M. Uehara, J. Suzuki, K. Sekine, *Journal of Power Sources* 129 (2004) 96-100.
- [30] L. Ji, X. Zhang, *Electrochemistry Communications* 11 (2009) 1146-1149.
- [31] M. Liang, L. Zhi, *Journal of Materials Chemistry* 19 (2009) 5871-5878.



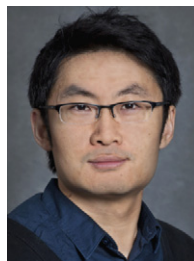
Liwen Ji received his B.S. degree in Materials Chemistry from Lanzhou University in 2001 and M.S. degree in Polymer Chemistry and Physics from Zhejiang University in 2004. After nearly two and a half years' research experience in Shanghai Institute of Organic Chemistry, he started to study at North Carolina State University and received his Ph.D. degree in Fiber and Polymer Science in 2009 under the supervision of Professor Xiangwu Zhang. He is currently a Materials Postdoctoral Fellow working with Dr. Yuegang Zhang at the Molecular Foundry, Lawrence Berkeley National Laboratory. His research focuses on novel nanostructures for advanced energy storage and conversion systems.



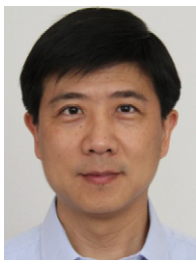
Ariel Ismach received his Ph.D. in Chemistry from the Weizmann Institute of Science under the supervision of Prof. Ernesto Joselevich in the Materials and Interfaces Department working on surface-induced alignment of single-wall carbon nanotubes. He then spent two years as a Postdoctoral Researcher in the University of California at Berkeley and the Lawrence Berkeley National Laboratory working with Prof. Jeffrey Bokor and Dr. Yuegang Zhang. He joined Prof. Rodney Ruoff's group at the University of Texas at Austin in 2011 and he is currently working on the synthesis and characterization of 2D materials.



Zhongkui Tan received his Bachelor's degree in Physics at Peking University in 2001; Master degree in Physics (condensed matter) at Peking University in 2004; Ph.D. in Physics (nanoelectronics) at Stony Brook University in 2010. During 2010-2011, he worked as a Postdoctoral Fellow at the Molecular Foundry (graphene electronics), Lawrence Berkeley National Lab. He is currently an Engineer at Lam Research.



Shidi Xun is a Postdoctoral Fellow at Lawrence Berkeley National Laboratory (LBNL) in Berkeley, USA. He completed his Ph.D. in Chemistry from Carleton University, Canada. His current research is focused on the development of materials for lithium ion batteries.



Yuegang Zhang is currently a Career Staff Scientist at the Molecular Foundry of Lawrence Berkeley National Laboratory. He received his B.S. and M.S. degrees in Physics at Tsinghua University, Ph.D. in Materials Science at the University of Tokyo. After his Ph.D. in 1996, he conducted research on nanotubes and nanowires at NEC Fundamental Research Labs and Stanford University. He joined Intel in 2002 as a Senior

Scientist, and had been the leader of the Intel Carbon Nanotube Research Project and the Chairman of Intel Memory Strategic Research Sector. He also serves as a Committee Member of ITRS Emerging Research Device/Materials Working Group. His current research interests are nanomaterials synthesis and applications in nanoelectronics and energy conversion/storage.